JACS
JOURNAL OF THE AMERICAN CHEMICAL SOCIETY
Article
pubs.acs.org/JACS

High-Throughput Profiling of Peptide–RNA Interactions Using Peptide Microarrays

Jaeyoung Pai,[†] Taejin Yoon,[†] Nam Doo Kim,[‡] Im-Soon Lee,[§] Jaehoon Yu,*[,∥] and Injae Shin*[,†]

[†]National Creative Research Center for Biofunctional Molecules, Department of Chemistry, Yonsei University, Seoul 120-749, Korea
[‡]New Drug Development Center, Daegu-Gyeongbuk Medical Innovation Foundation, Daegu 706-010, Korea
[§]Department of Biological Sciences, Konkuk University, Seoul 143-701, Korea
[∥]Department of Chemistry and Education, Seoul National University, Seoul 151-742, Korea

Supporting Information

ABSTRACT: A rapid and quantitative method to evaluate binding properties of hairpin RNAs to peptides using peptide microarrays has been developed. The microarray technology was shown to be a powerful tool for high-throughput analysis of RNA–peptide interactions by its application to profiling interactions between 111 peptides and six hairpin RNAs. The peptide microarrays were also employed to measure hundreds of dissociation constants (K_d) of RNA–peptide complexes. Our results reveal that both hydrophobic and hydrophilic faces of amphiphilic peptides are likely involved in interactions with RNAs. Furthermore, these results also show that most of the tested peptides bind hairpin RNAs with submicromolar K_d values. One of the peptides identified by using this method was found to have good inhibitory activity against TAR–Tat interactions in cells. Because of their great applicability to evaluation of nearly all types of RNA–peptide interactions, peptide microarrays are expected to serve as robust tools for rapid assessment of peptide–RNA interactions and development of peptide ligands against RNA targets.

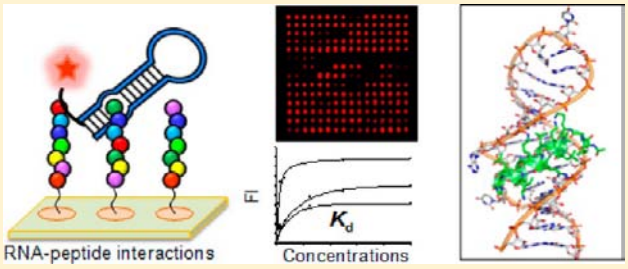

INTRODUCTION

RNA molecules play a pivotal role in most events taking place in cells. These biomolecules often have a hairpin (or stem-loop) motif as one of their most frequently occurring secondary structural features.[1] It has been known that RNA hairpins, through interaction with RNA binding proteins, are involved in various biological processes, including modulation of gene expression, and mRNA localization and translation. Recently discovered microRNAs, which play a role in regulation of gene expression,[2] also frequently possess hairpin secondary structures, albeit they lack three-dimensional structural information.[1] Because RNA binding proteins recognize hairpin motifs as part of physiological changes, it is expected that hairpin RNAs are promising targets in an approach to treat various diseases.

Hairpin RNAs form grooves as do double-stranded DNAs, which can provide binding pockets. Several attempts have been made to identify small molecules that bind to hairpin RNAs.[3,4] However, most of the substances have been found to associate only weakly with RNAs due to the fact that the large surface area (1100–1500 A^2) of the RNA groove is difficultly covered by small molecules (150 A^2).[5] In contrast, peptides are potential ligands with high affinities against hairpin RNAs, and they can be used to regulate RNA–protein interactions in biological and pharmaceutical applications. In fact, biophysical and biochemical studies have shown that α-helical peptides containing both natural and unnatural amino acids are reasonable ligands for hairpin RNAs.[6,7] Unfortunately, the currently used methods for analysis of RNA–peptide recognition events, such as fluorescence anisotropy, NMR spectroscopy, and X-ray crystallography, are not amenable to rapid analysis of large numbers of events. As a consequence of the limitations of the current techniques, a pressing need exists to develop other powerful tools that can be utilized to evaluate multiple RNA–peptide interactions in a high-throughput fashion.

In the studies described below, we employed peptide microarrays to probe RNA–peptide interactions because the microarray technology is a robust, reliable, and efficient technique for large-scale analysis of biochemical and biological events.[8,9] To date, peptide microarrays have been widely utilized for rapid assessment of protein–peptide recognition events,[10,11] large-scale determination of enzyme activities, and high-throughput profiling of substrate specificities of enzymes.[12−17] Furthermore, the microarray technology has become a promising diagnostic method because of its potential use to detect pathogen infections and for antibody diagnostics.[18,19] However, peptide microarrays remain underexploited as tools in analyzing binding events of hairpin RNAs to peptides. In the investigation described below, we have

Received: October 2, 2012
Published: October 30, 2012

   dx.doi.org/10.1021/ja309760g | J. Am. Chem. Soc. 2012, 134, 19287–19296

established a simple and robust method for probing peptide–RNA interactions in a microarray format (Figure 1). The results

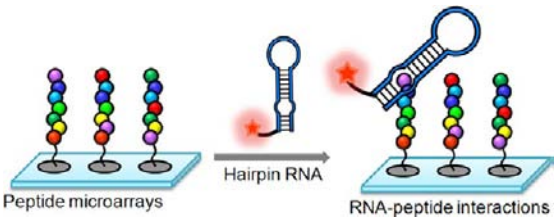

Figure 1. Peptide microarrays used for studies of RNA–peptide interactions. Peptide microarrays containing various peptides are probed with fluorophore-labeled hairpin RNAs.

of this effort demonstrate that peptide microarrays serve as powerful tools for rapidly profiling large numbers of RNA–peptide interactions and for measurements of their corresponding dissociation constants.

METHODS

Synthesis of C-Terminal Hydrazide-Linked Peptides and Cy3-Labeled Peptides. A series of C-terminal hydrazide-linked peptides were synthesized by using the Fmoc/tBu strategy on a Wang resin (0.9 mmol/g).[20] A solution of 4-nitrophenyl chloroformate (4 equiv) in CH_2Cl_2 was added to a Wang resin (0.9 mmol) in 9 mL of CH_2Cl_2 and 2,6-lutidine (8 equiv) at room temperature. After being shaken for 12 h, the resin was washed with 10% DMF in CH_2Cl_2 at least five times. Subsequently, a solution of hydrazine (5 equiv) and *N*,*N*-diisopropylethylamine (DIEA, 10 equiv) in DMF was added to the resin. After being shaken for 4 h, the resin was washed with DMF at least five times. An Fmoc amino acid (3 equiv) was manually coupled to the resin (10.0 μmol) for 3 h at room temperature in the presence of *N*,*N*,*N*′,*N*′-tetramethyl-*O*-(1*H*-benzotriazol-1-yl)uronium hexafluorophosphate (HBTU, 3 equiv), *N*-hydroxybenzotrizole (HOBt, 3 equiv), and DIEA (6 equiv). After each coupling reaction, a solution of DMF–DIEA–Ac_2O (0.5 mL, 2:2:1 (volume ratio)) was added to the resin, and then the mixture was shaken for 15 min to cap the unreacted amino group. The Fmoc group was removed by treatment with 20% piperidine in DMF, and the resin was washed with DMF and CH_2Cl_2 at least five times. Peptides assembled on the resin were cleaved from the solid support by treatment with 1 mL of a cleavage cocktail solution (trifluoroacetic acid (TFA):triisopropylsilane (TIS) = 49: 1 (v/v)) for 2 h at room temperature. Cleaved peptides were eluted from the resin by filtration and washed with TFA. A stream of nitrogen gas was used to remove TFA from the eluted peptide solution, and 1.5 mL of diethyl ether was added to the residue. The resulting gel-like solution was centrifuged at 13 000 rpm for 1 min at room temperature. After the supernatant was carefully discarded, the pellet was dissolved in DMSO (20 μL). Peptides were purified by preparative reversed-phase HPLC with a gradient of 5–100% CH_3CN (0.1% TFA) in water (0.1% TFA) over 60 min, and the purified products were characterized by MALDI-TOF MS (Table S1).

To prepare Cy3-labeled peptides, a solution of Cy3-NHS (20 μL, 100 mM in DMSO) and the C-terminal hydrazide-linked peptide (100 μL, 10 mM in DMSO) in 1 mL of sodium phosphate buffer (100 mM, pH 5.4) was stirred for 5 h at room temperature. Peptides were purified by using RP HPLC under the above elution conditions, and the purified products were characterized by MALDI-TOF MS (Table S1).

Preparation of the Epoxide-Derivatized Glass Slide. Amine-coated glass slides (Nuricell, GS nanotech, Seoul, South Korea) were immersed into 3% poly(ethylene glycol) diglycidyl ether in 10 mM $NaHCO_3$ (pH 8.3) for 30 min under gentle shaking. The resulting epoxide-derivatized slides were washed with water and then dried by purging with argon gas.

To prepare slides containing a long linker, the above epoxide-derivatized slides were immersed into 3% 4,7,10-trioxa-1,13-tridecanediamine in 10 mM $NaHCO_3$ (pH 8.3) for 3 h under gentle shaking. After the slides were washed with water, they were immersed into 3% poly(ethylene glycol) diglycidyl ether in 10 mM $NaHCO_3$ (pH 8.3) for 30 min under gentle shaking. The resulting slides were washed with water and then dried by purging with argon gas.

Construction of Peptide Microarrays. The C-terminal hydrazide-linked peptides were dissolved in 100 mM sodium phosphate buffer (pH 5.4) containing 40% glycerol. Aliquots of the solutions (10 μL, 0.5 mM) were placed into the wells of a 384-well plate. Each peptide (1 nL) from the 384-well plate was printed in duplicate at predetermined places on a epoxide-derivatized glass slide with a distance of 240 μm between the centers of adjacent spots by using a pin-type microarrayer (MicroSys 5100 PA, Cartesian Technologies). After completion of printing, the slide was placed into a humid chamber (55–60% relative humidity) at room temperature for 5 h. The slide was then divided into several blocks by using a compartmentalized plastic film that was coated with adhesive on one side (thickness: 0.1–0.2 mm) to avoid cross-contamination. The slide was washed three times with PBS buffer (pH 7.4) containing 0.1% Tween-20 under gentle shaking for 5 min. After the slide was dried by purging with argon gas, a solution (15–20 μL) of 10 mM $NaHCO_3$ (pH 8.3) containing 1% 2-aminoethanol was dropped onto the compartmented block and then left at room temperature for 30 min. The slide was washed three times with PBS buffer (pH 7.4) containing 0.1% Tween-20 under gentle shaking for 5 min. To obtain reproducible results, the fabricated peptide microarrays were immediately used.

Fluorescent Detection of RNA–Peptide Interactions on Peptide Microarrays. Solutions (15–20 μL) of 0.25 μM RNAs (RNAs purified by PAGE were purchased from Dharmacon) labeled by Dye 547 (Thermo Scientific) in 20 mM HEPES (pH 7.4) containing 1 mM $MgCl_2$, 5 mM KCl, 140 mM NaCl, and 0.05% Tween-20 were dropped onto each block compartmented by a plastic film and then incubated for 1 h at room temperature. The unbound RNAs were removed by washing the slide with PBS buffer containing 0.1% Tween-20 (30 mL, 3 min × 3). After the slide was dried by purging with argon gas, the slide was scanned using an ArrayWoRx biochip reader (Applied Precision, Northwest Issaquah, WA).

Determination of Dissociation Constants for RNA–Peptide Interactions Using Peptide Microarrays. The C-terminal hydrazide-linked peptides (111 peptides) were printed eight times at predetermined places onto the epoxide-derivatized glass slide with a distance of 270 μm between the centers of adjacent spots by using a pin-type microarrayer. Peptide microarrays were incubated with various concentrations of fluorophore-labeled RNAs (15–20 μL) in 20 mM HEPES (pH 7.4) containing 1 mM $MgCl_2$, 5 mM KCl, 140 mM NaCl, and 0.05% Tween-20 for 1 h at room temperature. The unbound RNAs were removed by washing the slide with PBS buffer containing 0.1% Tween-20 (30 mL, 3 min × 3). The slide was scanned using an ArrayWoRx biochip reader. The fluorescent intensity of each spot was quantified using ImaGine version 6.1 (BioDiscovery, Inc.). After the background intensity was subtracted, the fluorescence intensities of RNAs bound to peptides were averaged to obtain the signal intensity of each condition, and presented graphs were compiled by Origin Pro 8 software. Dissociation constants (K_d) were calculated by using the following equations:[21]

$$\mathrm{Fl} = \mathrm{Fl}_{max}[\mathrm{RNA}]_0/(K_d + [\mathrm{RNA}]_0)$$

where Fl_{max} is the maximum fluorescence intensity, Fl is the mean fluorescence intensity, and $[\mathrm{RNA}]_o$ is the initial concentration of RNA. All K_d values were the average of three independent experiments.

Measurement of Circular Dichroism (CD). CD measurements were performed at 20 °C on a JASCO model J-815 spectropolarimeter equipped with a Peltier thermostatted cell holder and running JASCO Spectra Manager software. Spectra were corrected from background contribution by subtracting control buffer spectra, and the CD signal was converted to mean residue ellipticity, $[\Theta]$, by $[\Theta] = \Theta_{obs}[\mathrm{MRW}/(10 \times l \times c)]$, where MRW is the mean residue weight (molecular mass divided by number of peptide bonds), l is path length in cm, and c is concentration in mg/mL.

Molecular Modeling. Molecular modeling of an RRE−peptide complex was performed on a 12-core Intel Zeon Linux workstation using a ZDOCK program (Accelrys Software). RRE RNA coordinates were taken from the structure of a complex of a HIV-1 Rev peptide with RRE RNA (PDB code 1ETG).[22] The original RRE and peptide sequences were modified using Discovery Studio 3.5. Each structure of RRE and peptide was subjected to 5000 iterations of steepest descent energy minimization using the molecular mechanics software CHARMM. Two minimized structures were docked to specify the residues involved in the RNA−peptide interaction. ZDOCK was used with 6° rotational sampling intervals to generate 2000 poses. Clusters of similar docking pose were determined, and the top-scoring cluster was selected as a structure of the peptide−RRE complex. The generated structure of a peptide−RRE complex was further subjected to steepest descent energy minimization using CHARMM to produce an energy minimized structure of the complex.

Cell Culture. HeLa cells were cultured in Dulbecco's modified Eagle's medium (DMEM, Invitrogen) supplemented with 10% (v/v) fetal bovine serum (FBS, Gibco), 100 units/mL penicillin (Gibco), and 100 μg/mL streptomycin (Gibco) in a humidified incubator with 5% CO_2 at 37 °C.

Luciferase Assay. Dual luciferase assays were performed using the dual luciferase assay system (Promega Corp., Madison, MI). All reagents were prepared as described by the manufacturer's protocol. Harvested cells were lysed with Luciferase Cell Lysis Buffer. Cell lysates (20 μL out of 30 μL total lysate per sample) were analyzed for firefly luciferase activity by adding 20 μL of firefly reaction buffer. Furthermore, Renilla luciferase activity was measured by adding 20 μL of Renilla reaction buffer. Luminescence was measured from a 384-well plate by using VictorX5 multilabel plate reader (Perkin-Elmer). Luciferase luminescence intensity was divided by Renilla luminescence intensity to compensate for the variation of the transfection efficiency. Data are presented as normalized fold change, with enhancement of luciferase activity with negative control (transfection without pCEP4-tat, an effecter plasmid) normalized to 1.

Microscopy. HeLa cells (ca. 2×10^4) were plated on 18 mm round glasses in a 24-well plate in DMEM (10% FBS, 100 units/mL penicillin, and 100 μg/mL streptomycin) and cultured for 12 h to obtain ca. 30% confluent. Cell culture medium was replaced by DMEM medium containing the Cy3-labeled peptide (20 μM). After 24 h incubation at 37 °C, the cells were washed five times with DMEM medium to remove the residual Cy3-labeled peptide. Hoechst 33342 (1 μg/mL, Pierce) was added to the cell culture to stain the nucleus. After 15 min incubation at 37 °C, cells were washed three times with PBS buffer, and the round glasses seeded with cells were mounted upside down on a glass slide. Live cells were imaged at 630× magnification using confocal microscopy (LSM 510 META, Carl Zeiss).

Data Analysis and Statistics. Luciferase assay results are based on more than three independent experiments, and data are presented as mean ± s.d., and statistical analysis was performed using one-way ANOVA. For cluster analysis of peptide−RNA interactions, the average linkage clustering was performed to generate cluster images using MultiExperiment Viewer (MeV).[23]

RESULTS AND DISCUSSION

Peptide Design. We previously reported that amphiphilic peptides, which preferentially form helical structures, tightly associate with hairpin RNAs.[24] On the basis of the observation made in an earlier investigation, in the current study we selected the peptide sequence of LKKLLKLLKKLLKLKG (**1**), which binds to hairpin RNAs with a high affinity, as a standard ligand. A series of peptides were designed to investigate the effect of deletion or substitution of amino acids in **1** on peptide binding to hairpin RNAs (Figure 2a). The N-terminal amino acids (peptides **2**−**5**) were sequentially deleted from **1** to examine the effect of peptide length on RNA binding. In addition, Lys residues in **1** were replaced by Ala (peptides **6**−**11**) and Gln (peptides **12**−**32**) to evaluate the effect of positively charged amino acid residues on RNA binding. Substitution of Gln for Lys was carried out to probe the effect of introducing a residue that has a hydrophilic side chain with α-helical propensity that has a size similar to that of Lys but does not possess the ability to participate in ionic interactions with the phosphate backbone of RNAs.

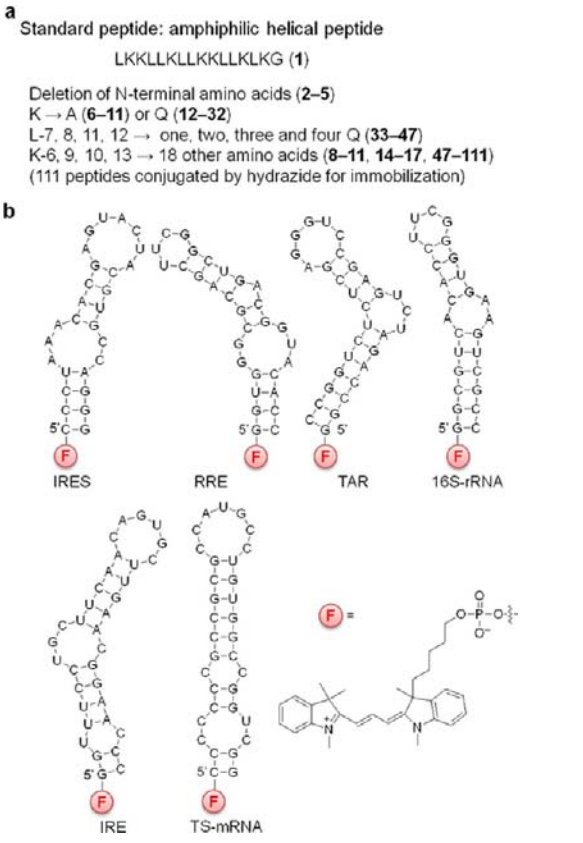

Figure 2. Sequences of (a) peptides and (b) fluorophore (F)-labeled hairpin RNAs at the 5′ terminus used in this study (IRES, internal ribosome entry site of domain IV of hepatitis C virus; RRE, HIV Rev responsive element; TAR, HIV transactivation response element; IRE, iron responsive element; and TS-mRNA, thymidylate synthase mRNA).

Furthermore, to understand the effect of hydrophobic residues in peptides on RNA binding, Leu in the middle region (Leu-7, 8, 11, 12) of **1** was replaced by one (peptides **33**−**36**), two (peptides **37**−**42**), three (peptides **43**−**46**), and four Gln (peptide **47**). Moreover, to systematically investigate the effect of Lys in peptides on RNA binding, Lys residues in the middle region (Lys-6, 9, 10, 13) of **1** were singly replaced by 18 other amino acids (peptides **8**−**11**, **14**−**17**, **47**−**111**) except Cys.

Peptide Microarrays. Because the peptides possess several nucleophilic Lys side chains, a chemoselective immobilization method is required for site-specific peptide attachment to modified solid surfaces. We previously developed an immobilization technique, which relies on selective and efficient reaction between hydrazide groups and epoxide-derivatized surfaces under weakly acidic conditions (pH 5−6), that is selective even when nucleophilic Lys and Cys residues are present in peptides.[25,26] Using this immobilization strategy, peptide microarrays containing 111 different peptides were prepared in this study employing peptides with the C-terminal

hydrazide group, which were synthesized on a hydrazide-linked solid support by using a standard solid-phase peptide synthesis protocol (Scheme 1 and Table S1).

Scheme 1. C-Terminal Hydrazide-Conjugated Peptides Are Assembled on a Solid Support by Using a Standard Solid-Phase Peptide Synthesis Protocol (AA = Amino Acid)

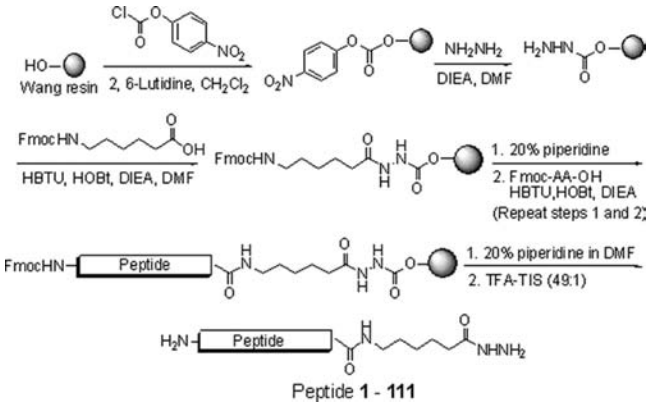

To examine the effect of tether length on RNA binding, two types of epoxide-derivatized glass slides, containing different tether lengths (short and long tethers), were prepared (Figure S2). For this purpose, 11 hydrazide-conjugated peptides (**1**–**11**, 0.5 mM, pH 5.5) were printed in duplicate on each epoxide-coated surface by using a robotic pin-type microarrayer. The abilities of the peptides to bind RNAs were then probed by incubating the resultant peptide microarrays with 0.25 μM hairpin RRE RNA labeled with a fluorophore at the 5′ terminus (Figure 2b).[27] In this step, a solution of RRE containing various concentrations (0–0.5%) of Tween-20 was applied to peptide microarrays to reduce nonspecific adsorption of RNAs. Analysis of the microarray data shows that tether length does not greatly influence peptide binding to RRE (Figure S3). Thus, an epoxide slide containing a short tether was used in further studies because of its ease of preparation. The data also indicate that addition of 0.05–0.5% Tween-20 to RNA solutions is crucial for obtaining reproducible and reliable microarray analyses (Figure S3).

Profiling RNA–Peptide Interactions Using Peptide Microarrays. To evaluate their interactions with hairpin RNAs, 111 peptides (0.5 mM, pH 5.5), with sequences described above and containing C-terminal hydrazide groups, were printed in duplicate on the epoxide-derivatized surface. The resulting peptide microarrays were probed with six fluorophore-labeled hairpin RNAs, including IRES,[28] RRE,[27] TAR,[29] 16S-rRNA,[30] IRE,[31] and TS-mRNA,[32] in the presence of 0.05% Tween-20 (Figure 2b). Mean fluorescence intensities were determined using data from five-independent experiments (<10% variation in fluorescence intensity) and scored as positive signals. The combined data set is presented as a graph of fluorescence intensities or a colored heatmap (Figure 3 and Figure S4).

Results obtained from microarray experiments show that IRES and RRE RNAs strongly interact with peptides, TAR and 16S-rRNA associate with peptides with median binding affinities, and IRE and TS-mRNA recognize peptides with significantly reduced affinities. The observations demonstrate that binding affinities of peptides to hairpin RNAs depend on the sequence and shape of RNAs. Specifically, the lengths of the peptides influence RNA binding affinities (Figure 3). Peptides containing one (**2**) or two amino acid deletions (**3**) at the N-terminus bind to RNAs with similar affinities as does **1**. However, deletion of three (**4**) and four amino acids (**5**) at the N-terminus leads to conspicuously reduced binding to RNAs. In particular, it appears that the remarkably decreased binding affinity to RNAs of peptide **5** is a consequence of the deletion of two of positively charged Lys residues and its poor α-helicity (Figure S5). The results indicate that peptide sequences with minimum 14 amino acids are required for strong binding to hairpin RNAs. Moreover, a single substitution of Ala (**6**–**11**) or Gln (**12**–**17**) for Lys in **1** has a little influence on RNA binding.

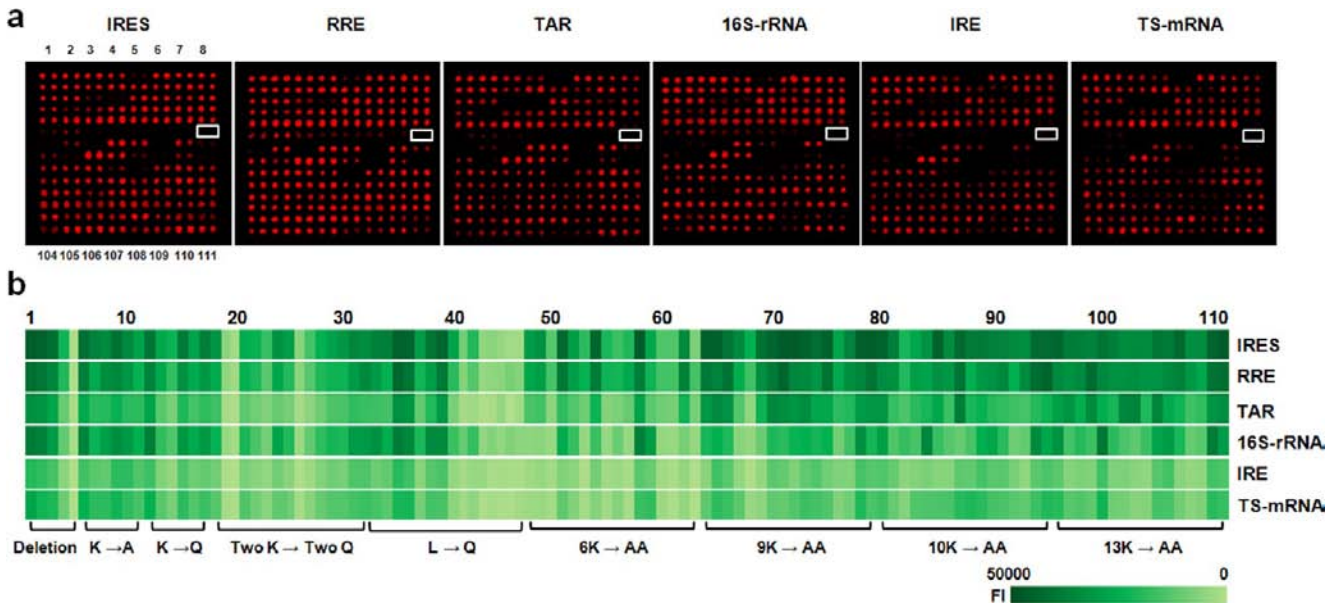

Figure 3. Peptide microarrays containing 111 peptides probed with six hairpin RNAs (0.25 μM). (a) Fluorescent images of peptide microarrays incubated with RNAs (a white box indicates spots printed with buffer solutions as a control). (b) Heatmap of 111 peptides against a panel of six hairpin RNAs (Fl = fluorescence intensity). The color ruler is shown at the bottom.

dx.doi.org/10.1021/ja309760g | J. Am. Chem. Soc. 2012, 134, 19287–19296

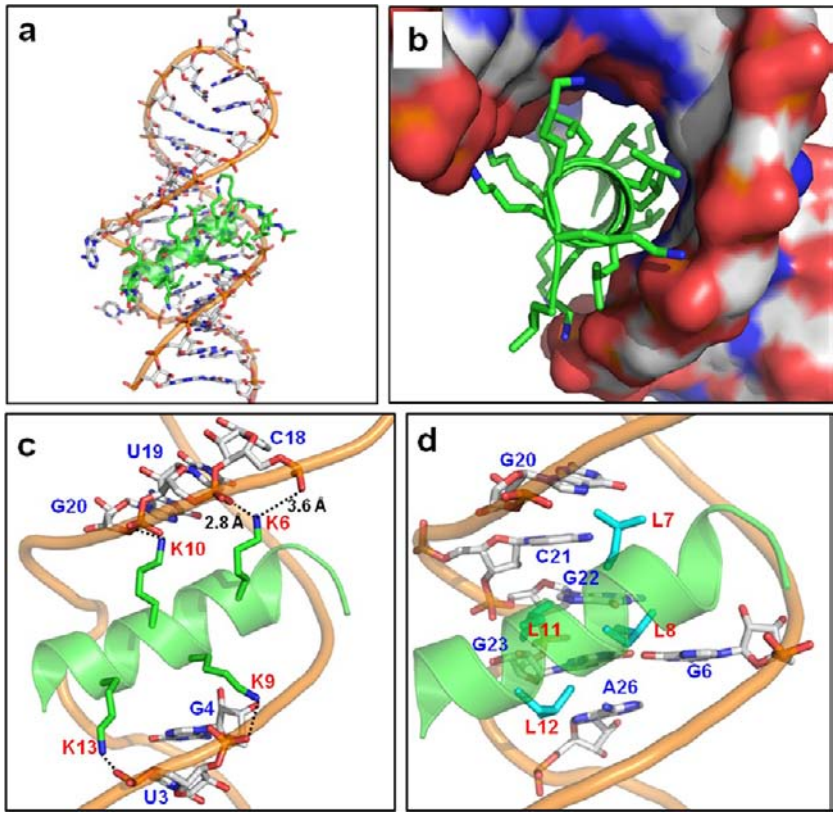

Figure 4. Molecular models of the RRE–peptide **1** complex. (a) Overall binding mode of RRE RNA to **1** (green: peptide **1**). (b) Side view of the solvent-accessible surface of the major groove of RRE complexed with **1**. (c) Binding mode of Lys-6, 9, 10, and 13 in **1** to phosphate groups of RRE. Lys-6 interacts with two phosphate groups of RRE in a bidentate mode. (d) Binding mode of Leu-7, 8, 11, and 12 in **1** to the major groove of RRE. Side chains of these leucine residues interact with several bases in the major groove of RRE through van der Waals contacts.

Substitution at the 2 position (peptides **6**, **12**) does not affect RNA binding; however, peptides (**7**, **8**, **13**, **14**) substituted at the 6 position display slightly reduced binding affinities to RNAs in comparison with **1**. Interestingly, peptides **18**–**32** with double Gln substitution bind to RNAs with more significantly decreased binding affinities than do those (**12**–**17**) with a single Gln substitution. This finding suggests that Lys residues play a large role in RNA binding through ionic interactions.[33]

Analysis of the microarray data obtained for peptides **33**–**47**, in which hydrophobic Leu residue(s) is replaced by one to four Gln, shows that the single mutation in peptides **33**–**36** has a little effect on RNA binding, and peptides **37**–**42** with double mutations have different binding affinities to RNAs that depend on the position of substitution. More striking is the observation that all peptides (**43**–**47**) with triple and quadruple mutations bind to RNAs with markedly reduced affinities. This result suggests that hydrophobic Leu residues are involved in RNA binding.[22,34] Finally, inspection of the microarray data for peptides **48**–**111**, in which Lys is replaced by other amino acids, reveals that peptides **48**–**63** substituted at the 6 position recognize RNAs with distinctly decreased binding affinities as compared to those (**64**–**111**) substituted at the 9, 10, or 13 positions. This phenomenon indicates that Lys at the 6 position is critical for RNA binding. In these peptide subsets, substitution of negatively charged Asp or Glu leads to attenuated RNA binding affinities due presumably to electrostatic repulsions between negatively charged residues and the phosphate groups of the RNAs.[33] According to the results of binding studies, peptides (**2**, **3**) with deletion of N-terminal one or two amino acids, peptides (**6**, **12**) with Ala or Gln substitution at the 2 position, and peptides (**35**, **36**) with a single substitution of Gln for Leu bind to RNAs with high affinities similarly to **1**.

To understand the effect of peptide α-helicity on RNA binding, CD spectra of 19 peptides (**1**, **10**, **16**, **80**–**95**), mutated at the 10 position, were measured (Figure S6). Comparison of the CD data and microarray derived binding properties shows that no significant correlation exists between α-helicity and binding affinity in singly substituted peptides. Taken together, the findings demonstrate that both the position and the nature of substituted amino acid(s) have an effect on the binding properties of peptides to hairpin RNAs, and that both hydrophobic and hydrophilic faces of peptides are likely involved in interactions with hairpin RNAs.

To gain information on the mode of peptide binding to hairpin RNAs, molecular docking studies were performed with a representative complex of a hairpin RNA and a peptide. Because the structure of a complex of RRE RNA with a helical Rev peptide is known,[22] the binding mode of peptide **1** to RRE RNA was explored. An analysis of the docking model suggests that **1** binds to the RRE major groove (Figure 4a), which is relatively deep and narrow, and that both hydrophilic and hydrophobic faces of **1** are mostly located at the surface of the major groove (Figure 4b). Moreover, Lys residues in the central region of the helical peptide **1** are involved in electrostatic interaction with RRE between the positively charged Lys side chains and the RNA phosphate backbone (Figure 4c). In particular, the results of the molecular modeling study show that Lys-6 in peptide **1** interacts with two phosphate groups of RRE in a bidentate mode, a phenomenon that is found in

dx.doi.org/10.1021/ja309760g | J. Am. Chem. Soc. 2012, 134, 19287–19296

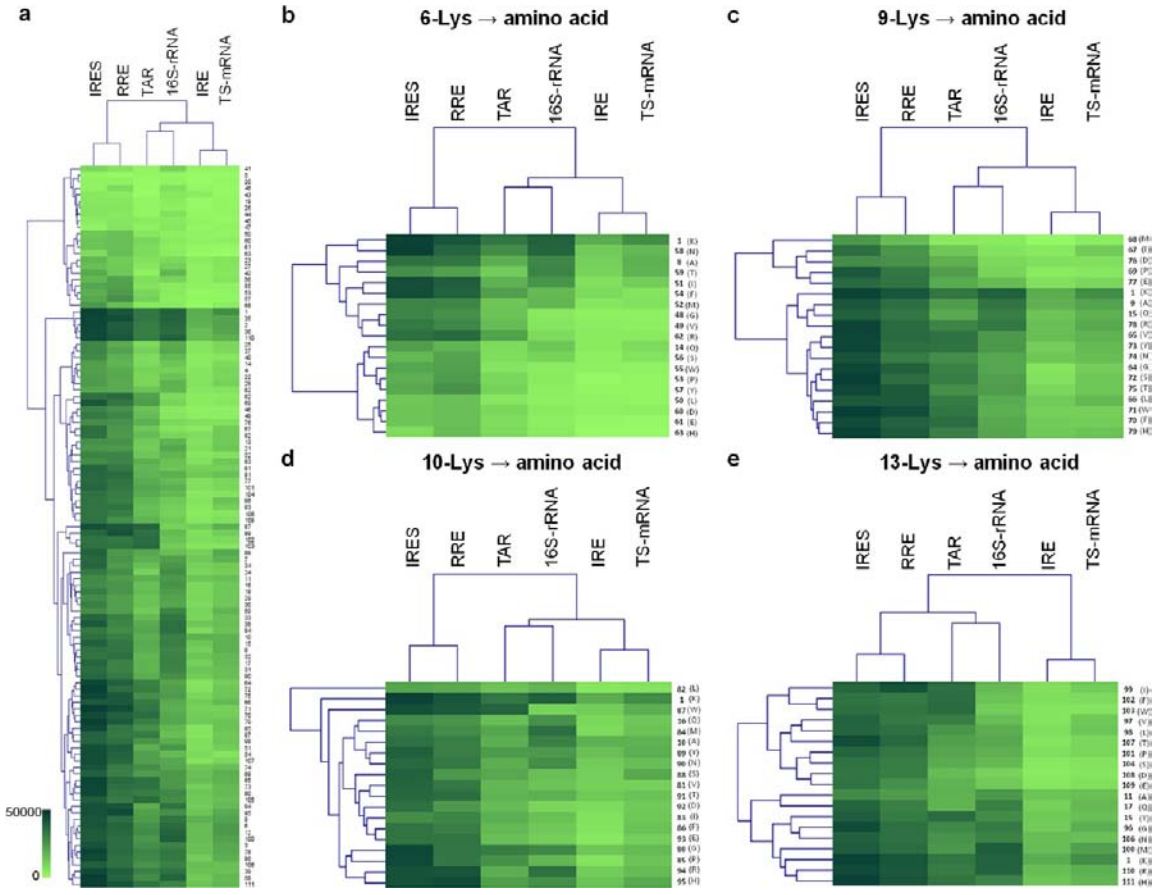

Figure 5. Average linkage hierarchical cluster analysis. Target RNAs are arrayed along the *x*-axis, and each peptide is arrayed along the *y*-axis. Clustering analysis was carried out using MultiExperiment Viewer software. The image is presented as a hierarchical tree. The tree structures indicate the degree of similarity of RNAs or peptides as a function of the height of the lines connecting profiles. Average linkage clustering was performed both across the RNA panels and across (a) a full set of peptides, and (b)−(e) subsets of peptides in which Lys at the 6, 9, 10, or 13 position was replaced by 18 other amino acids. The color ruler is shown at the left. Amino acids in parentheses are indicated by their single letter code.

structures of known DNA−protein or RNA−protein complexes.[33,35] The presence of this structural feature suggests that Lys-6 is important for RNA binding. In addition, it appears that the hydrophobic side chains of Leu-7, 8, 11, and 12 associate with bases in the major groove of RRE through hydrophobic interactions (or van der Waals contacts), a phenomenon that is also well-known for protein−DNA and protein−RNA interactions (Figure 4d).[36,37] Taken together, the molecular modeling studies suggest that both hydrophilic and hydrophobic faces are involved in RNA binding, which is consistent with the microarray data presented above.

Cluster Analysis of Peptide Binding to Hairpin RNAs. To compare peptide binding patterns against hairpin RNAs, six RNAs were hierarchically clustered according to the complete binding profile obtained from peptide microarray experiments. Average linkage cluster analysis was performed using hierarchical clustering software to group the data based on similarities among profiles of RNAs (*x*-axis) and peptides (*y*-axis). This analysis affords the hierarchical tree shown in Figure 5, which represents a classification on the basis of peptide binding of the RNA panels. Cluster analysis reveals that hairpin RNAs have distinct peptide binding profiles with strong binding RNAs (IRES and RRE) grouped closely together and weak binding RNAs (IRE and TS-mRNA) forming a sister pair, as do median binding RNAs (TAR and 16S-rRNA). The results of this analysis suggest that the peptide binding preferences of the grouped RNAs are similar (Figure 5a). In addition, the generally stronger binding peptides are more closely related to one another than they are to other groups, with the weaker peptides being grouped close together.

Cluster analysis of peptide binding data from each peptide subset containing Lys replacements at positions 6, 9, 10, and 13 by 18 other amino acids was also carried out for the RNA panel (Figure 5b−e). Four peptide subsets display distinct clustering patterns, indicating that the positions of substitution in the peptides affect their RNA binding properties. The most striking feature gleaned from this analysis is that peptides with replacements of Lys-6 by other amino acids reside together in overall weak binding (the bottom region), strong but nonspecific (or promiscuous) binding (the top region), and selective binding (the upper central region) groups (Figure 5b).[38] Most of the amino acids found in the selective region have hydrophobic side chains, indicating that substitution of hydrophilic Lys for hydrophobic amino acids in peptides increases binding specificity at the expense of binding affinity. The cluster analysis presented here provides information that potentially can be used when designing selective peptide ligands against hairpin RNA targets.

Quantitative Analysis of Peptide−Hairpin RNA Interactions Using Peptide Microarrays. In contrast to other conventional technologies, such as SPR spectroscopy, fluorescence anisotropy, and isothermal titration calorimetry,

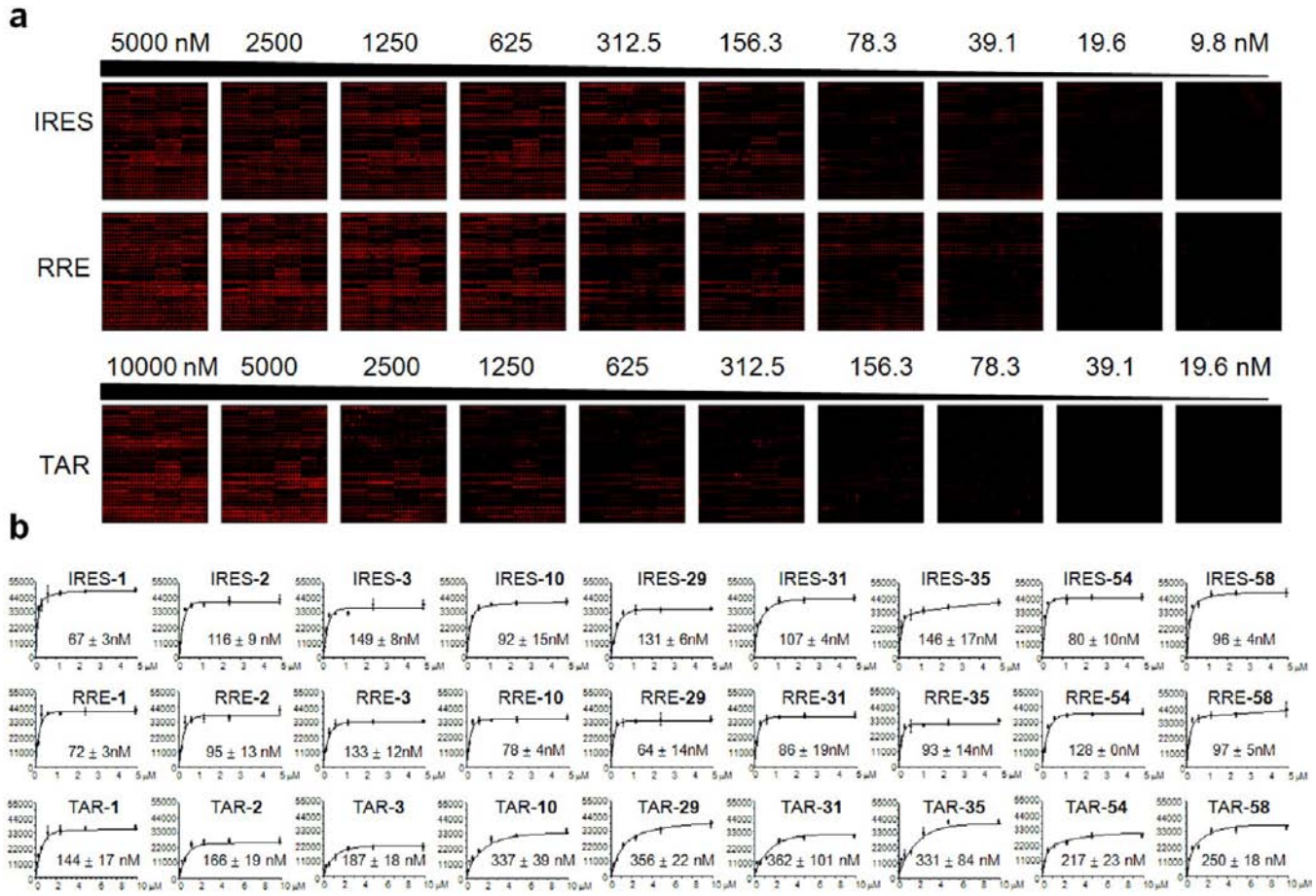

Figure 6. Determination of dissociation constants (K_d) for hairpin RNA–peptide interactions using peptide microarrays. (a) Fluorescent image of peptide microarrays probed with 10 different concentrations of fluorophore-labeled RNAs. (b) Graphs showing fluorescence as a function of peptide concentration for 27 of the selected RNA–peptide interactions. Data were analyzed on the basis of three independent experiments and presented as mean ± s.d.

microarray-based methods are known to serve as powerful methods for the rapid and simultaneous measurement of dissociation constants (K_d) for large numbers of protein–ligand interactions.[26,39] Thus, peptide microarrays were utilized to determine K_d values for more than 300 peptide–RNA interactions. Because nonspecific interactions of RNAs with peptides immobilized on surfaces linearly increase with increasing RNA concentrations, IRES, RRE, and TAR RNAs, which have relatively strong binding affinities to peptides, were employed for this study. 111 peptides (0.5 mM) were printed eight times on epoxide-derivatized surfaces, and the peptide microarrays were then probed with 10 concentrations of each fluorophore labeled RNA. K_d values were determined by the equation in Methods. The results show that most of curves fit well to the equation (coefficient of determination $R^2 \geq 0.9$). As a result, the microarray method can be used to perform 26 640 interaction measurements and obtain 333 K_d values (Figure 6, Tables S2–S4 and Figures S7–S9). The observations show that a majority of peptides bind to hairpin RNAs with submicromolar K_d values, and the strongly binding peptides have a few tens of nanomolar K_d values, indicating that most of the tested peptides associate with hairpin RNAs with strong binding affinities.

Inhibition of TAR–Tat Interactions by Peptides in Cells. To examine whether peptides used in the present study regulate RNA–protein interactions in cells, a cell-based assay system was employed in which TAR–Tat-mediated transcriptional activation is monitored by using a firefly luciferase reporter gene.[40] In this system, binding of RNA polymerase II to the complex of TAR with the Tat protein initiates transcription of a firefly luciferase gene, leading to increase in its expression level (Figure 7a).[41] However, if the TAR–Tat interaction is blocked by a competitive RNA binding peptide inhibitor, the expression level of the firefly luciferase reporter will be attenuated. To test this possibility, HeLa cells were cotransfected with three plasmids, including a reporter plasmid containing a firefly luciferase gene (pHIV-1-LTR-luc), an effecter plasmid containing a Tat gene (pCEP4-tat), and an internal control plasmid (pRL-SV40) containing a Renilla luciferase gene. As a negative control, HeLa cells were cotransfected with only pHIV-1-LTR-luc and pRL-SV40, which do not lead to Tat-mediated transcriptional activation of a firefly luciferase gene.

Four peptides (denoted as **1**′, **20**′, **37**′, **47**′) without a hydrazide linker at the C-terminus were investigated to determine their effect on inhibition of Tat-mediated transcriptional activation of firefly luciferase. HeLa cells were separately incubated with each of the four peptides (5 and 20 μM) from 2 h before transfection to 24 h after transfection with plasmids (pHIV-1-LTR-luc, pCEP4-tat, and pRL-SV40). In the absence of a peptide, firefly luciferase activity increased 16-fold as compared to the control (Figure 7b). In contrast, firefly

dx.doi.org/10.1021/ja309760g | J. Am. Chem. Soc. 2012, 134, 19287–19296

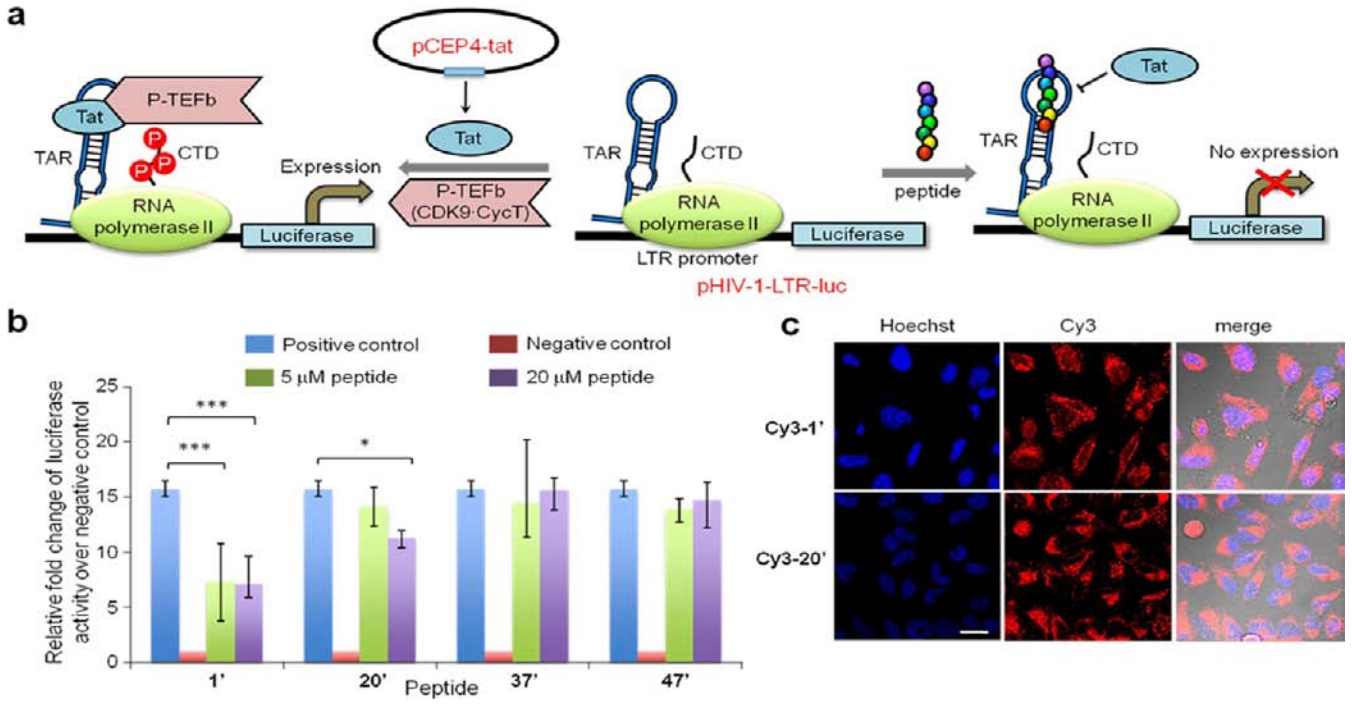

Figure 7. Effect of RNA binding peptides on TAR-Tat-mediated transcription in cells. (a) Cell-based assay system of transcriptional activation of a firefly luciferase reporter. Cells are cotransfected with a reporter plasmid (pHIV-1-LTR-luc) and an effecter plasmid (pCEP4-tat). During transcription, RNA polymerase II assembles on the HIV LTR (long terminal repeat) promoter with TAR RNA, followed by recruitment of P-TEFb (a complex of CDK9 with CycT) by Tat protein. CDK9 of P-TEFb hyperphosphorylates C-terminal domain (CTD) of RNA polymerase II, leading to expression of luciferase. However, the peptide binds to TAR to inhibit binding of Tat to TAR. This leads to suppression of transcriptional activation of a luciferase gene. (b) HeLa cells were preincubated with selected peptides (5, 20 μM) for 2 h. The cells were cotransfected with pHIV-1-LTR-luc and pCEP4-tat in the presence of the same concentrations of peptides. After transfection, cells were incubated with the same concentrations of peptides for 24 h. Relative luciferase activity was determined by firefly luciferase activity (reporter) relative to Renilla luciferase activity (internal control). Analysis of the data is based on more than three independent experimental observations (error = s.d.). ***$P < 0.001$; *$P < 0.05$. (c) Cellular uptake of Cy3-labeled peptides. HeLa cells were incubated with 20 μM Cy3-labeled **1**′ or **20**′ at 37 °C for 24 h. Live cell images were analyzed for determining cell permeability of the peptides by using confocal microscopy (bar = 20 μm). Hoechst was used to stain the nucleus.

luciferase activity was reduced by approximately 50% by treatment of cells with tight binding peptide **1**′, whereas treatment with the weak binding peptide **20**′ (mutation of Lys-2 and -9 in **1**′ to Gln) caused only a small decrease in activity. However, peptide **37**′ and **47**′ with substitution of two and four Gln for Leu show negligible inhibitory activity against firefly luciferase.

Cell permeability of peptides could affect their inhibitory activities in cells. To test this possibility, efficiency of cellular uptake of peptides was examined using Cy3-labeled peptides, which were prepared by coupling of C-terminal hydrazide conjugated peptides with Cy3-NHS (*N*-hydroxysuccinimide) ester. HeLa cells were incubated with 20 μM Cy3-labeled peptides for 24 h, and live cell images were recorded by using confocal microscopy to probe cell permeability of peptides. Image analysis shows that whereas peptide **1**′ and **20**′ internalize into cells to a similarly large degree (Figure 7c), peptides **37**′ and **47**′ with Gln substitutions enter cells to only a slight degree (Figure S10). This result indicates that the lack of bioactivity of peptide **37**′ in cells, despite its high binding affinity to TAR RNA, is a consequence of its inefficient cell permeability. In contrast, lower potency of peptide **20**′ in cells results from its weak binding affinity to TAR RNA. Taken together, the results of microarray-based profiling of RNA–peptide interactions show that it can be used reliably in the in vivo studies. However, it should be noted that the differential cell permeability of peptides should be considered when in vivo systems are employed.

CONCLUSION

The association of RNA binding proteins with hairpin motifs of RNAs plays a role in regulating a variety of physiological and pathological processes.[42] Therefore, RNA binding substances are valuable biological probes that can be employed to gain a better understanding of biological processes and to prevent the onset of various diseases. It has been shown that α-helical peptides bind to the hairpin structures of RNAs with a high affinity.[6] However, the prediction of the binding properties of helical peptides to hairpin RNAs is a complicated and difficult task. As a consequence, systematic studies for RNA–peptide interactions are necessary to gain a detailed understanding of these biomolecular recognition events as well as to identify tight and selective binding peptide ligands against hairpin RNA targets. In this context, technologies that enable the high-throughput analysis of RNA–peptide interactions are extremely important because individual measurements of many RNA–peptide interactions are both time and labor consuming.

In the investigation described above, we developed an efficient and powerful tool to rapidly evaluate binding properties of hairpin RNAs toward peptides. Although peptide microarrays have been utilized previously to elucidate various biological and biochemical events,[9−17] use of the microarrays to explore binding of peptides to RNAs in this format has not

been reported to date. By using peptide microarrays, we were able to profile interactions of six hairpin RNAs with 111 peptides, containing systematic amino acid replacements or deletions. The results obtained from this analysis suggest that both position and nature of the substituted amino acids significantly influence the binding affinities of peptides to hairpin RNAs. In addition, this microarray technology was also applied in a technique to measure more than 300 dissociation constants, a task that would be difficult by other conventional analytic methods. Most of the peptides were observed to bind to hairpin RNAs with submicromolar affinities, and strong binding peptides have a few tens of nanomolar K_d values. One peptide, which had a high binding affinity against TAR RNA and efficient cell permeability, was shown, by using a luciferase-based cell assay, to inhibit the TAR−Tat protein interaction significantly. Rapid identification and usage as a plausible ligand against a certain target RNA are definitely merits of peptide microarrays that were constructed in this work.

This finding points out a meritorious feature of peptide microarrays when they are applied to rapid identification of inhibitors of target RNA. Ultimately, this technique will aid in the identification of translational modulators that target RNA or of biochemical probes for functional studies of RNAs in cells. Importantly, due to the fact that RNA-binding peptides serve as promising leads in the treatment of various diseases, we envisage that microarray-based technologies will be useful in furthering an understanding of RNA−protein-mediated biological processes as well as the development of pharmacological agents.

■ ASSOCIATED CONTENT

Supporting Information

Experimental procedure and sequence of peptides, MS data for the synthesized peptides, HPLC profiles of peptides, CD spectra for peptides, preparation of epoxide-derivatized glass slides, effect of tether lengths on binding of RNA to peptides, quantitative analysis of fluorescence intensity of peptide microarrays probed with RNAs, and dissociation constants determinations. This material is available free of charge via the Internet at http://pubs.acs.org.

■ AUTHOR INFORMATION

Corresponding Author

injae@yonsei.ac.kr; jhoonyu@snu.ac.kr

Notes

The authors declare no competing financial interest.

■ ACKNOWLEDGMENTS

We thank Sejin Yang for early involvement in the project. This was supported by grants from the National Creative Research Initiative, WCU (R32-2008-000-10217-0), and NRL (20110028483) programs (NRF).

■ REFERENCES

(1) Svoboda, P.; Di Cara, A. *Cell. Mol. Life Sci.* **2006**, *63*, 901−918.
(2) (a) Hermann, T. *Curr. Opin. Struct. Biol.* **2005**, *15*, 355−366. (b) Chang, T. C.; Mendell, J. T. *Annu. Rev. Genomics Hum. Genet.* **2007**, *8*, 215−239. (c) Bartel, D. P. *Cell* **2009**, *136*, 215−233.
(3) (a) Gallego, J.; Varani, G. *Acc. Chem. Res.* **2001**, *34*, 836−843. (b) Renner, S.; Ludwig, V.; Boden, O.; Scheffer, U.; Gobel, M.; Schneider, G. *ChemBioChem* **2005**, *6*, 1119−1125. (c) Battiste, J. L.; Mao, H.; Rao, N. S.; Tan, R.; Muhandiram, D. R.; Kay, L. E.; Frankel, A. D.; Williamson, J. R. *Science* **1996**, *273*, 1547−1551.
(4) (a) Tor, Y. *ChemBioChem* **2003**, *4*, 998−1007. (b) Renner, S.; Ludwig, V.; Boden, O.; Scheffer, U.; Göbel, M.; Schneider, G. *ChemBioChem* **2005**, *6*, 1119−1125. (c) DeJong, E. S.; Chang, C. E.; Gilson, M. K.; Marino, J. P. *Biochemistry* **2003**, *42*, 8035−8046.
(5) Leeper, T. C.; Athanassiou, Z.; Dias, R. L. A.; Robinson, J. A.; Varani, G. *Biochemistry* **2005**, *44*, 12362−12372.
(6) (a) Das, C.; Frankel, A. D. *Biopolymers* **2003**, *70*, 80−85. (b) Heaphy, S.; Dingwall, C.; Ernberg, I.; Gait, M. J.; Green, S. M.; Karn, J.; Lowe, A. D.; Singh, M.; Skinner, M. A. *Cell* **1990**, *60*, 685−693. (c) Zhou, Q.; Sharp, P. A. *Science* **1996**, *274*, 605−610.
(7) Lee, Y.; Hyun, S.; Kim, H. J.; Yu, J. *Angew. Chem., Int. Ed.* **2008**, *47*, 134−137.
(8) Fodor, S. P. A.; Read, J. L.; Pirrung, M. C.; Stryer, L.; Lu, A. T.; Solas, D. *Science* **1991**, *251*, 767−773.
(9) Katz, C.; Levy-Beladev, L.; Rotem-Bamberger, S.; Rito, T.; Rudiger, S. G. D.; Friedler, A. *Chem. Soc. Rev.* **2011**, *40*, 2131−2145.
(10) (a) Frank, R. *J. Immunol. Methods* **2002**, *267*, 13−26. (b) Stiffler, M. A.; Chen, J. R.; Grantcharova, V. P.; Lei, Y.; Fuchs, D.; Allen, J. E.; Zaslavskaia, L. A.; MacBeath, G. *Science* **2007**, *317*, 364−369.
(11) (a) Tomizaki, K. Y.; Usui, K.; Mihara, H. *ChemBioChem* **2005**, *6*, 783−799. (b) Tomizaki, K.-y.; Usui, K.; Mihara, H. *FEBS J.* **2010**, *277*, 1996−2005. (c) Usui, K.; Tomizaki, K. Y.; Mihara, H. *Methods Mol. Biol.* **2009**, *570*, 273−284.
(12) (a) Thiele, A.; Stangl, G. I.; Schutkowki, M. *Mol. Biotechnol.* **2011**, *49*, 283−305. (b) Salisbury, C. M.; Maly, D. J.; Ellman, J. A. *J. Am. Chem. Soc.* **2002**, *124*, 14868−14870. (c) Zhu, Q.; Uttamchandani, M.; Li, D.; Lesaicherre, M. L.; Yao, S. Q. *Org. Lett.* **2003**, *5*, 1257−1260.
(13) (a) Houseman, B. T.; Huh, J. H.; Kron, S. J.; Mrksich, M. *Nat. Biotechnol.* **2002**, *20*, 270−274. (b) Su, J.; Bringer, M. R.; Ismagilov, R. F.; Mrksich, M. *J. Am. Chem. Soc.* **2005**, *127*, 7280−7281.
(14) Schutkowski, M.; Reimer, U.; Panse, S.; Dong, L. Y.; Lizcano, J. M.; Alessi, D. R.; Schneider-Mergener, J. *Angew. Chem., Int. Ed.* **2004**, *43*, 2671−2674.
(15) Kohn, M.; Gutierrez-Rodriguez, M.; Jonkheijm, P.; Wetzel, S.; Wacker, R.; Schroeder, H.; Prinz, H.; Niemeyer, C. M.; Breinbauer, R.; Szedlacsek, S. E.; Waldmann, H. *Angew. Chem., Int. Ed.* **2007**, *46*, 7700−7703.
(16) (a) Uttamchandani, M.; Wang, J.; Li, J.; Hu, M.; Sun, H.; Chen, K. Y.-T.; Liu, K.; Yao, S. Q. *J. Am. Chem. Soc.* **2007**, *129*, 7848−7858. (b) Sun, H. Y.; Lu, C. H. S.; Uttamchandani, M.; Xia, Y.; Liou, Y. C.; Yao, S. Q. *Angew. Chem., Int. Ed.* **2008**, *47*, 1698−1702. (c) Wu, Hao, Ge, J.; Yang, P.-Y.; Wang, J.; Uttamchandani, M.; Yao, S. Q. *J. Am. Chem. Soc.* **2011**, *133*, 1946−1954.
(17) Doezé, R. H. P.; Maltman, B. A.; Egan, C. L.; Ulijn, R. V.; Flitsch, S. L. *Angew. Chem., Int. Ed.* **2004**, *43*, 3138−3141.
(18) Duburcq, X.; Olivier, C.; Malingue, F.; Desmet, R.; Bouzidi, A.; Zhou, F. L.; Auriault, C.; Gras-Masse, H.; Melnyk, O. *Bioconjugate Chem.* **2004**, *15*, 307−316.
(19) Andresen, H.; Grotzinger, C.; Zarse, K.; Kreuzer, O. J.; Ehrentreich-Forster, E.; Bier, F. F. *Proteomics* **2006**, *6*, 1376−1384.
(20) Hyun, S.; Kim, H. J.; Lee, N. J.; Lee, K. H.; Lee, Y.; Ahn, D. R.; Kim, K.; Jeong, S.; Yu, J. *J. Am. Chem. Soc.* **2007**, *129*, 4514−4515.
(21) Kuno, A.; Uchiyama, N.; Koseki-Kuno, S.; Ebe, Y.; Takashima, S.; Yamada, M.; Hirabayashi, J. *Nat. Methods* **2005**, *2*, 851−856.
(22) Battiste, J. L.; Mao, H. Y.; Rao, N. S.; Tan, R. Y.; Muhandiram, D. R.; Kay, L. E.; Frankel, A. D.; Williamson, J. R. *Science* **1996**, *273*, 1547−1551.
(23) Saeed, A. I.; Hagabati, N. K.; Braisted, J. C.; Liang, W.; Sharov, V.; Howe, E. A.; Li, J. W.; Thiagarajan, M.; White, J. A.; Quackenbush, J. *Methods Enzymol.* **2006**, *411*, 134−193.
(24) Lee, S. J.; Hyun, S.; Kieft, J. S.; Yu, J. *J. Am. Chem. Soc.* **2009**, *131*, 2224−2230.
(25) Lee, M. R.; Shin, I. *Angew. Chem., Int. Ed.* **2005**, *44*, 2881−2884.
(26) (a) Park, S.; Shin, I. *Org. Lett.* **2007**, *9*, 1675−1678. (b) Park, S.; Lee, M. R.; Shin, I. *Nat. Protoc.* **2007**, *2*, 2747−2758.
(27) Lacourciere, K. A.; Stivers, J. T.; Marino, J. P. *Biochemistry* **2000**, *39*, 5630−5641.
(28) Kieft, J. S. *Trends Biochem. Sci.* **2008**, *33*, 274−283.

(29) Cao, H.; Tamilarasu, N.; Rana, T. M. *Bioconjugate Chem.* **2006**, *17*, 352−358.
(30) Ryu, D. H.; Litovchick, A.; Rando, R. R. *Biochemistry* **2002**, *41*, 10499−10509.
(31) Canzoneri, J. C.; Oyelere, A. K. *Nucleic Acids Res.* **2008**, *36*, 6825−6834.
(32) Tavares, T. J.; Beribisky, A. V.; Johnson, P. E. *RNA* **2009**, *15*, 911−922.
(33) (a) Dertinger, D.; Uhlenbeck, O. C. *RNA* **2001**, *7*, 622−631. (b) García-García, C.; Draper, D. E. *J. Mol. Biol.* **2003**, *331*, 75−88.
(34) Hyun, S.; Na, J.; Lee, S. J.; Park, S.; Yu, J. *ChemBioChem* **2010**, *11*, 767−770.
(35) Ha, S. C.; Lokanath, N. K.; Van Quyen, D.; Wu, C. A.; Lowenhaupt, K.; Rich, A.; Kim, Y. G.; Kim, K. K. *Proc. Natl. Acad. Sci. U.S.A.* **2004**, *101*, 14367−14372.
(36) Luscombe, N. M.; Laskowski, R. A.; Thornton, J. M. *Nucleic Acids Res.* **2001**, *29*, 2860−2874.
(37) Puglisi, J. D.; Chen, L.; Blanchard, S.; Frankel, A. D. *Science* **1995**, *270*, 1200−1203.
(38) Greenbaum, D. C.; Arnold, W. D.; Lu, F.; Hayrapetian, L.; Baruch, A.; Krumrine, J.; Toba, S.; Chehade, K.; Bromme, D.; Kuntz, I. D.; Bogyo, M. *Chem. Biol.* **2002**, *9*, 1085−1094.
(39) Jones, R. B.; Gordus, A.; Krall, J. A.; MacBeath, G. *Nature* **2006**, *439*, 168−174.
(40) Lalonde, M. S.; Lobritz, M. A.; Ratcliff, A.; Chamanian, M.; Athanassiou, Z.; Tyagi, M.; Wong, J. L.; Robinson, J. A.; Karn, J.; Varani, G.; Arts, E. J. *PLoS Pathog.* **2011**, *7*, e1002038.
(41) Ott, M.; Geyer, M.; Zhou, Q. *Cell Host Microbe* **2011**, *10*, 426−435.
(42) Hermann, T. *Angew. Chem., Int. Ed.* **2000**, *39*, 1891−1905.